Real-Time Simulation of EV Grid Integration with Internet-Inspired Charging Control

Emin Ucer[1], Nuh Erdogan[2], Shahinur Rahman[1], Mithat C. Kisacikoglu[1]
[1]Dept. of Electrical and Computer Eng., The University of Alabama, Tuscaloosa, AL
[2]MaREI Centre, Environmental Research Institute, University College Cork, Ireland

***Abstract*—Analyzing realistic EV-grid integration (EVGI) with available simulation tools is cumbersome due to the software overhead associated with offline simulation. Alternatively, real-time hardware platforms are becoming convenient means for testing and evaluating systems before field implementation. This study presents a digital implementation of an EVGI model in real-time on a multi-core processor based simulation platform. Furthermore, an Interned-inspired EV charging control algorithm is proposed in a decentralized fashion to prevent congestion related problems in a residential distribution grid. The impact of the proposed EV charging control on the IEEE 37-node test system is evaluated through the real-time analysis. The developed controller results show promise for extension to any utility-interfaced power electronics system. Real-time simulation implementation requirements and challenges in the context of EVGI are also discussed.**

I. Introduction

Massive EV-grid integration (EVGI) is on the horizon. This phenomenon will bring new challenges such as grid congestion, severe voltage deviations, and transformer overloading [1]–[8]. To address these problems in EV charging, the proposed solutions include centralized [9]–[12] and distributed approaches [13]–[18]. Centralized control methods are more established in the literature and used to optimize certain parameters in the system. On the other hand, distributed control utilizes local measurements as much as possible so that the need for a communication network that may suffer from network-related limitations such as complexity, latency, data security, and privacy is minimized.

EVGI control must ensure a fair and efficient utilization of the distribution system capacity among EV users while avoiding the grid congestion for sustainable mass integration. In its early days, the Internet also experienced similar congestion problems as the number of end-users drastically increased [19]. Mainstream transfer protocol (TCP) was developed as a solution and is still being implemented at end-points using local measurements [20]. This protocol uses the additive increase and multiplicative decrease (AIMD) algorithm for congestion control [21]. AIMD is basically an event-triggered mechanism that takes control actions whenever a congestion occurs in the network. Previous studies also tried to adapt the AIMD control to EV charging [15]–[18]. These studies lack detecting the grid congestion with only local variables and require some sort of communication overhead. Authors previously investigated implementing AIMD via heavily using local variables [22]–[26]. In this study, we impelemented AIMD algorithm in a real-time simulation environment.

Design, testing, and analysis of EV charging controllers are currently handled using off-line simulation. One of the major approach is to use phasor-based simulation that considers magnitude and phase calculation of voltages and currents in a steady-state operation mode [27]. This approach does not capture transient events that might occur in the power grid. On the other hand, time-based real-time simulation (RTS) capture very fast transients using dedicated processors. This allows to calculate instantaneous current and voltage waveforms [27]. Parallel hardware platforms can perform the RTS in which the system is sampled at the same time length as real-world time [28]. Such an environment is essential to do hardware-in-the-loop (HIL) testing of AIMD control to evaluate the real integration challenges of the control algorithm, a step that should be verified before field implementation. A real-time emulated EV-grid model, therefore, allows us to analyze the EV charging and other loads in the distribution system under a wide range of situations in a non-destructive environment.

In this study, an EV-grid model is emulated on a multi-core real-time simulator. The impact of proposed AIMD-based EV charging algorithm on the distribution grid are tested and analyzed in real-time. HIL testing results are presented to show the impact of the proposed charging algorithm on the actual grid. Section II presents EV-grid integration test system. The IEEE 37-node test feeder is used as a benchmark. Section III introduces the proposed AIMD-based EV charging algorithm. Section IV presents the experimental RTS test setup. Section V presents the testing results, followed by the concluding remarks in Section VI.

II. EV Grid Integration System Description

A. Distribution Grid Modeling

To emulate an EVGI system, this study uses the IEEE 37-node test feeder as a benchmark [29]. The modeled grid is a 2.5 MVA, 230 kV/4.8 kV, 37-bus, three-phase balanced network. EV charging loads are incorporated in the system

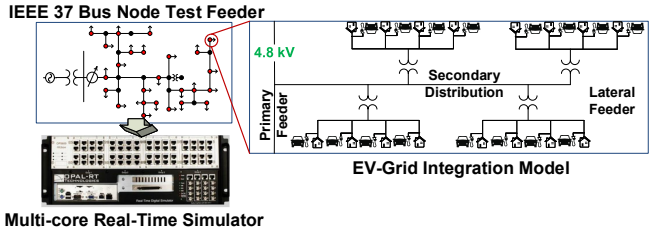

Figure 1: EV-grid integration system model.

This paper has been accepted for presentation in the 3^{rd} E-Mobility Power System Integration Symposium, Dublin, Ireland, on October 14, 2019.

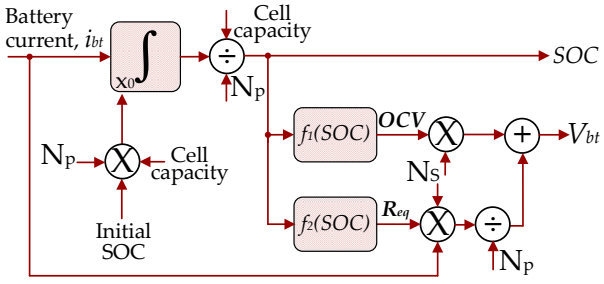

Figure 2: Implemented battery model.

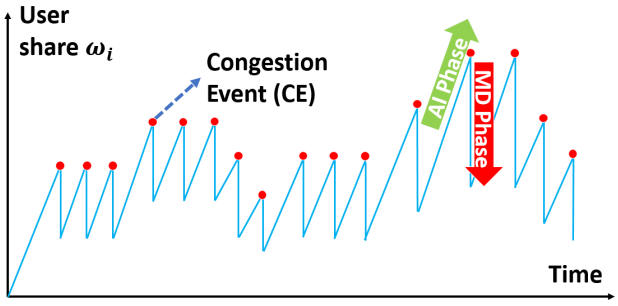

Figure 3: Time-domain waveform of a user share under the AIMD operation.

in parallel with conventional residential loads as shown in Fig. 1. In accordance with the test feeder configuration, the loads are connected to the buses through a ground transformer rated at 25 kVA and 4.8 kV/120-240 V split-phase. Each bus includes four inner nodes to which four residential and EV loads are connected in parallel. There are a total of 10 neighborhoods and 160 residential customers in the model[1]. The EVGI model is developed and implemented in Matlab/SIMULINK environment while RT-LAB [30] is used to compile and run it on the target platform.

B. Household Load Modeling

A household load data generator is developed to create more realistic power consumption profiles for all houses in the model. 16 days of real power consumption data in one minute resolution was collected using publicly available e-Gauge meter data of a residential house [29]. There are 16 samples coming from 16-day household data for each minute, and we calculated the mean and standard deviation statistics of these samples. Then, we generated a new power value for each particular time interval from a Gaussian distribution function with the calculated mean and standard deviation. We repeated the process to generate a different power profile for each house in the model. As we only have active power consumption data currently, we considered a constant 0.9 power factor lagging operation in the simulation and kept the real power consumption the same. The future work will include more detailed household load modeling thanks to a new E-gauge meter installed to a real house in Alabama [31].

C. EV Battery Modeling

In this study, we developed a battery system model that is compatible to operate in real-time simulation environment. The implemented battery pack model is shown in Fig. 11.

The battery model is comprised of an open-circuit cell voltage (OCV) in series with an equivalent internal resistance (R_{eq}) that both change as a function of the cell state of charge (SOC), i.e. f_1 and f_2. The initial SOC of the battery pack and cumulative battery current (I_{bt}) generate the instantaneous SOC at each time step, which is used to calculate R_{eq} and OCV. Voltage drop due to R_{eq} and OCV together produce voltage across the battery (V_{bt}) at each time step. In this study, a 24.8 Ah, 3.7 V nominal, baseline Li-on battery cell is used to form the battery pack model for each EV. Battery packs are modeled such that they have a rated capacity of 60 kWh and maximum charging current of 30 A. Number of cells that are in series (N_s) is 93, and number of parallel strings (N_p) is seven. All the EVs are modeled with the same parameters to preserve fairness in the performance assessment of the proposed AIMD algorithm.

[1]The original model is downsized to realize real-time simulation as detailed in Section IV.

III. Internet-Inspired Charging Control Algorithm

Fair allocation of a limited capacity among many users while making sure that the system will operate in a safe and stable way is a core problem in many engineering disciplines. The Internet's standards and protocols that have led to its ever-increasing growth are the results of years of debates and research around this very problem. The early days of the today's Internet suffered from the congestion challenges as the number of users greatly increased [19]. The observed congestion collapses [32], [33] made it necessary to develop a solution to ensure the stability of the system as well as the fair and efficient utilization of the available capacity. Given the size of the Internet, a possible solution would be better realized at end-nodes in a decentralized, plug-and-play manner without the need for a centralized controller to keep track of every newly added end-point. Therefore, the AIMD algorithm [21] was first introduced as a congestion avoidance solution, and it is still serving as the Internet's congestion avoidance solution today.

We will first explain the mechanism of the general AIMD algorithm and propose a counterpart algorithm for EV charging control. The algorithm is triggered by the capacity event (CE) that takes place when the network is congested due to high utilization by users. Every user increases their share in the network (i.e. charging power for EV network) linearly until a CE occurs. This phase is called the additive increase (AI) phase. In case of CE, users decrease shares by scaling them down allowing for reallocation of the available capacity. This is the multiplicative decrease (MD) phase. A typical time-domain waveform of a user share under the AIMD operation is illustrated in Fig. 3. The general model of the AIMD algorithm can be written as a piece-wise function as in (1), where w_i is the i^{th} user's share, α_i is the the increase parameter and $0 < \beta_i < 1$ is the decrease factor.

$$w_i(t+1) = \begin{cases} w_i(t) + \alpha_i & \text{if no CE happens} \\ w_i(t) \times \beta_i & \text{if CE happens} \end{cases} \quad (1)$$

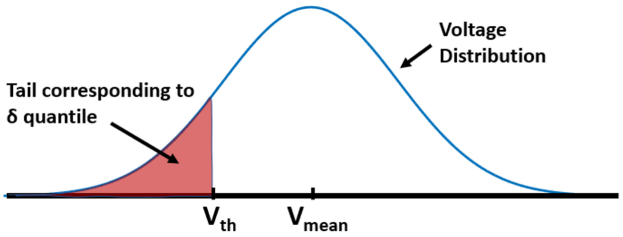

Figure 4: Computation of the threshold value using the statistics of the voltage distribution.

Algorithm 1 AIMD algorithm for EV charging network

Parameter: Increase parameter: $\alpha(t) > 0$
Parameter: Decrease parameter: $0 < \beta(t) < 1$
Input: Previous charging current: $I_i(t)$
Input: Node voltage: $V_i(t)$
Output: New charging current: $I_i(t+1)$

```
while SOC < 100% do
    Measure voltage: V = [V(1), V(2), ··· , V(t)]
    V_th,i = UpdateThreshold(V, δ)
    if V(t) > V_th,i and V(t) > V_min then
        I_i(t+1) = I_i(t) + α_i
    else
        I_i(t+1) = β_i × I_i(t)
    end if
end while
```

The Internet has an implicit congestion detection mechanism that allows users to detect congestion using their local information. This is accomplished by observing the statistics of packet round trip times (RTT) on a network link. If these times are measured to be much longer than an average timeout, this can mean a congested network for users. Similarly in a distribution network, end-nodes experience higher voltage drops as the grid is more loaded. These voltage drops can be translated into a power congestion when they are significant enough compared to the average voltage regime. When this average regime is learned, the users can take charging actions based on their local voltage measurements. Inspired by the Internet's congestion detection, we propose Algorithm 1 as a counterpart algorithm for EV charging. The algorithm takes voltage measurements over one-minute time interval and calculates a voltage threshold value equal to the δ quantile of the collected voltage data. This threshold essentially represents the learned average voltage regime and can be demonstrated in Fig. 4. In this study, we set δ equal to 0.25, which is also known as the 25^{th} percentile. V_{min} represents the minimum allowed utilization voltage, which is chosen to be 216 V RMS specified by ANSI C84.1-2016. The algorithm parameters α and β are set to 1 and 0.5, respectively.

IV. Real-time Simulation Platform Description

The choice of a real-time simulation platform is based on its performance, cost, and constraints imposed by the application. The performance is assessed by the computational time and accuracy. The constraint dictated by our application is mainly the system scale. Most of the actual real time simulation platforms have computational step times

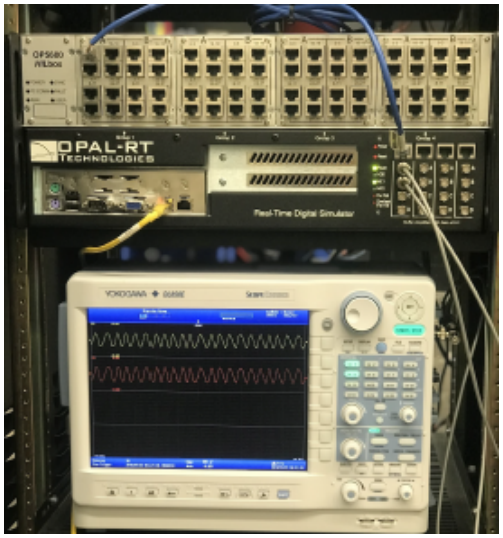

Figure 5: OP5600 real time simulation platform.

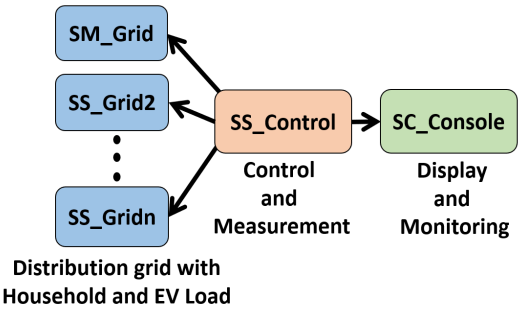

Figure 6: An overview of modelling a test system into several subsystems in RT-LAB Platform.

in the range of microseconds which will be sufficient to capture dynamics of an EVGI system which is in the range of milliseconds. In this study, a multi-core processor based target platform OPAL-RT OP5600 [30] is selected for the real-time execution of the developed EVGI model with respect to the above-mentioned considerations. The platform consists of 12 Intel processor cores @3.0 GHz that can be executed in parallel, including a SPARTAN-3 FPGA card as the I/O interface with 256 analog and digital I/O lines. Fig. 5 shows the set-up along with the real-time observation of system variables using a YOKOGAWA DL850E DAQ device.

An RTS requires that all computations in the model must be done in an interval equal to or less than the simulation time step size. The accuracy is another crucial aspect for the trustworthiness of the RTS results. Improving the accuracy based on utilization of detailed models increases the simulation computational time within each time step. However,

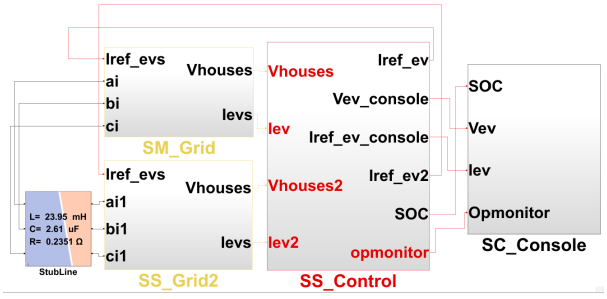

Figure 7: High-level system view of the model.

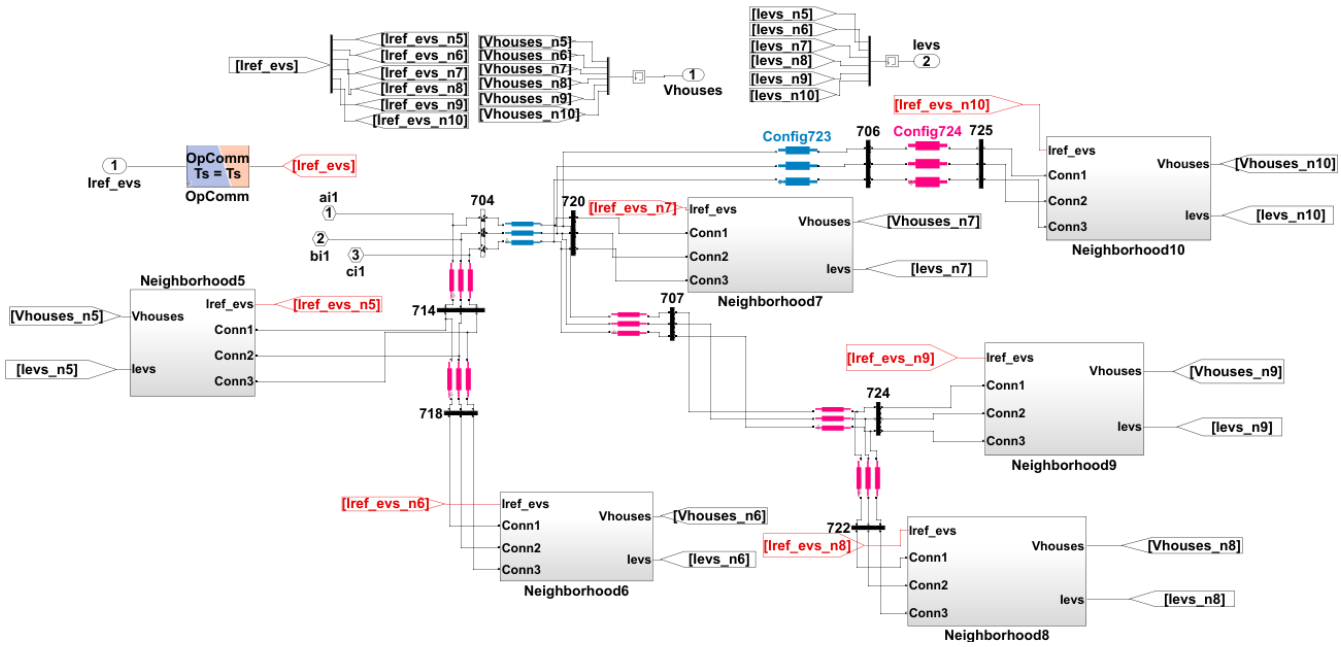

Figure 8: A part of the main feeder with 6 connected neighborhoods (SS-Grid2).

the growing need for a wider frequency bandwidth inherently requires a smaller simulation time step. Those lead to a trade-off between accuracy and frequency bandwidth for the RTS.

In the RT-LAB platform, the test system is divided and designed into several subsystems to enable parallel programming which reduces computational burden and distinguish computational blocks and input/output interface. This design configuration approach is summarized in Fig. 6. In our RT-LAB model, the IEEE 37-bus along with neighbourhood loads (household and EV) is designed into two subsystems (SM-Grid and SS-Grid2) to assign the computation load to different CPU cores and do parallel computing inside the cores of the target platform. The high-level overview of the RT-Lab model is shown in Fig. 7[2]. Stub-line block is used to make an interface between the signals of two subsystems. SS-Control subsystem, on the other hand, is built to implement the proposed AIMD charging control and provide measurements whereas SC-Console block displays the desired signals to the user.

The part of the main feeder where six neighborhoods are connected is shown in Fig. 8 (SS-Grid2). Further zooming in one of the neighborhoods, Fig. 9 shows individual blocks of houses that are connected with one another. Each of the house blocks are fed by a ground transformer rated at 25 kVA. Furthermore, Fig. 10 shows four houses powered by one ground transformer. Each of the houses has an EV as well as a regular household power consumption profile that was explained in Section II-B. Last, Fig. 11 shows household level implementation of power consumption in the RTS environment.

As explained above, the system scale and the proposed algorithm complexity in our study are computationally demanding. To have a proper simulation time step, the EVGI model has been executed for different time steps demanding various computational powers. The use of available computational power was optimized by decoupling the model into three parts within the RT-Lab software [30]. This makes it suitable for parallel programming where cores are assigned to each part separately and can run multiple instructions on a single die at the same time. To maintain the desired computational speed (i.e., simulation time step), the target uses five cores in parallel in our application. Considering dynamics, the calculation time step was tested with two different settings: (i) 250 μs and (ii) 500 μs. $T_s = 500$ μs resulted in individual core loading of 20% for SM-Grid, 42% for SS-Grid2, and 16% for SS-control. In contrast, for a higher fidelity simulation if $T_s = 250$ μs, then every individual core utilization almost doubles. In the future, we will further optimize the design so that number of neighborhoods increase from 10 to 26. However, the challenge is as more EVs are connected to the grid, the simulator might violate the RTS system requirement in terms of the time step that will lead to data losses and inaccuracy. One way to avoid this issue is to further increase simulation time step. We can run the full system model at a time step of one ms. However, increasing simulation time step decreases the numerical resolution which is undesirable in time domain simulation to preserve accuracy. We will find a good compromise between the accuracy and optimized complexity of the EVGI system.

V. RTS Results and Analysis

A day-long real-time simulation (e.g., 24h) has been finally performed. When presenting the results, we employed the following methodology is employed: we selected three houses with respect to the distance to the main substation (i.e., the closest, the intermediate, and the farthest) to verify the controller performance. The node voltages, EV currents,

[2]Note that the individual variables in Figs 7–11 are out of scope and will not be introduced in the paper. These figures aim to show how RTS platform is deisgned and how it works.

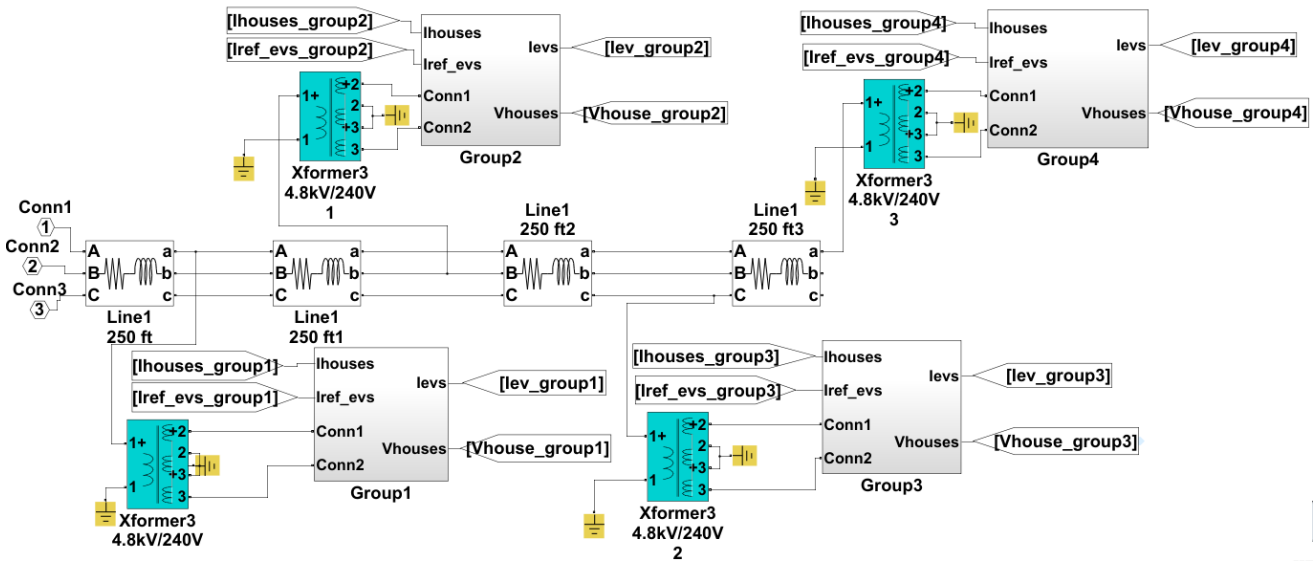

Figure 9: The neighborhood modeling with four house groups each powered by a 25kVA ground transformer.

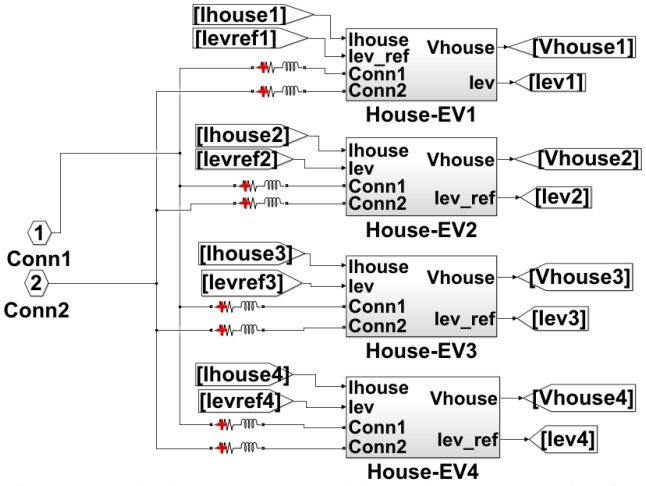

Figure 10: The house group model. Each group contains four houses connected to the same transformer through a service cable.

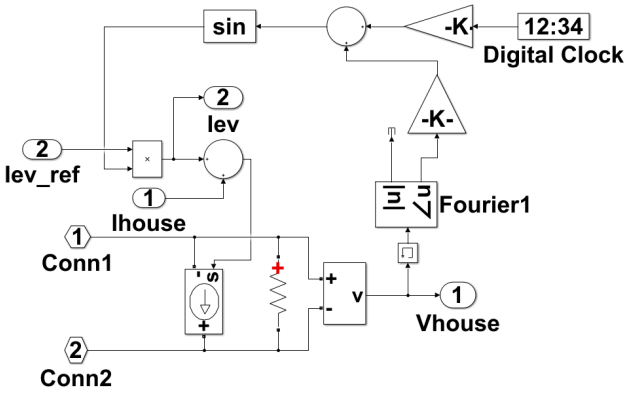

Figure 11: Household and EV load modeling. A controlled current source is used to model these dynamic loads.

and their SOCs have been measured through the analog outputs of the platform as shown in Fig. 5. We also recorded these signals for three distinct nodes in 0.01 sec resolution through the DataLogger feature provided with RT-LAB from release version 11.3 upwards.

EVs start arriving to the neighborhoods after 4PM of simulation time. Since the simulation is performed in real-time, the actual voltage waveforms are sinusoidal. Therefore, the farthest node voltage is provided in Fig. 12 to show one sample of the actual voltage waveform for a single node for verification. Furthermore, the node voltages of the three chosen houses for the first four hours are shown in Fig. 13. The threshold voltages are computed on the fly based on the voltage measurements collected during every minute. The voltage drops and variations typically increase as we go further away from the substation, which can also be seen in Fig. 13. This causes distant nodes to experience higher voltage deviations and therefore go into the MD phase more frequently. Consequently, the average charging currents (and thus powers) of these nodes will be less compared to closer nodes.

Fig. 14 compares the RMS current waveforms of the three chosen EV nodes with AIMD-based charging control. The average current values are calculated as 16.2 A, 15.3 A, and 11.7 A for the closest, intermediate, and furthest nodes, respectively. This shows that the closer nodes take advantage of higher voltages and less variations, and therefore get to charge their vehicles at higher powers whereas the further nodes suffer from the deviations more and have to curtail their powers. This phenomenon is also an expected observation of the decentralized AIMD and usually known as the *proportional fairness*. We should also note that the furthest node's voltage is maintained at the minimum service voltage of 216V. This shows that its charging power must have been further reduced not to violate the utility voltage requirement.

The resulted charging powers have also an impact on the charging times. Fig. 15 shows the SOC values of the chosen vehicles in percentage with respect to time. The all three vehicles start charging at nearly the same SOC level (85%) and receive charge for four hours. Due to the difference between the average charging powers, the furthest EV was

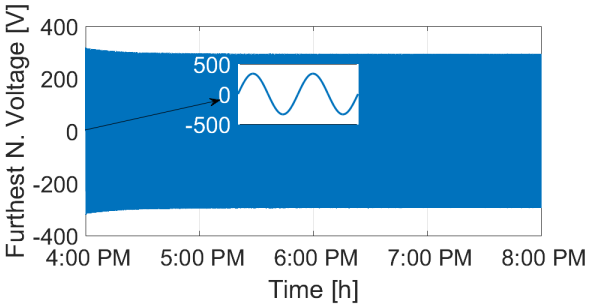

Figure 12: The farthest real-time node voltage measured during four hour simulation.

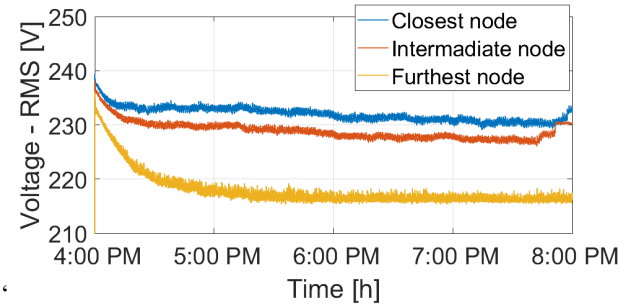

Figure 13: RMS voltages of the selected three nodes.

able to get charged up to little over 95% while the closer EVs get fully charged in four hours[3]. The algorithm can also be modified by a pre-defined policy in favour of the further nodes by changing the parameters such as α and β, and the quartile constant δ. However, this requires further information regarding the location of the nodes and the overall grid state, and therefore makes it more centralized.

VI. Conclusion and Future Work

In this study, a real-time simulation of an EVGI model has been used to test Internet-inspired charging control on a multi-core processor based parallel hardware platform. The impact of proposed EV charging algorithm on sharing the available capacity among users has been evaluated through RTS. We showed that a decentralized AIMD algorithm for EV charging based on local measurements can be implemented in real-time in time-domain without any stability problem. The algorithm resulted in considerably close charging powers for the nodes closer to the substation. The furthest node had to reduce its power due to experiencing higher voltage deviations and being closer to the minimum service voltage (proportional fairness). RTS system requirements and challenges in the context of EVGI have been also addressed. RTS platform provides an HIL testbed to evaluate the developed AIMD controller under a wide range of contingencies and extreme conditions in a nondestructive environment before field implementation. Future work will focus on further developing the grid model and introducing real EV charging hardware implementation using a grid simulator connected to the HIL platform described in this study. AIMD control will be tested using a power electronics converter connected to the grid simulator.

[3]It is important to note that CV charging is not implemented in this study and will be added to RTS in the future studies.

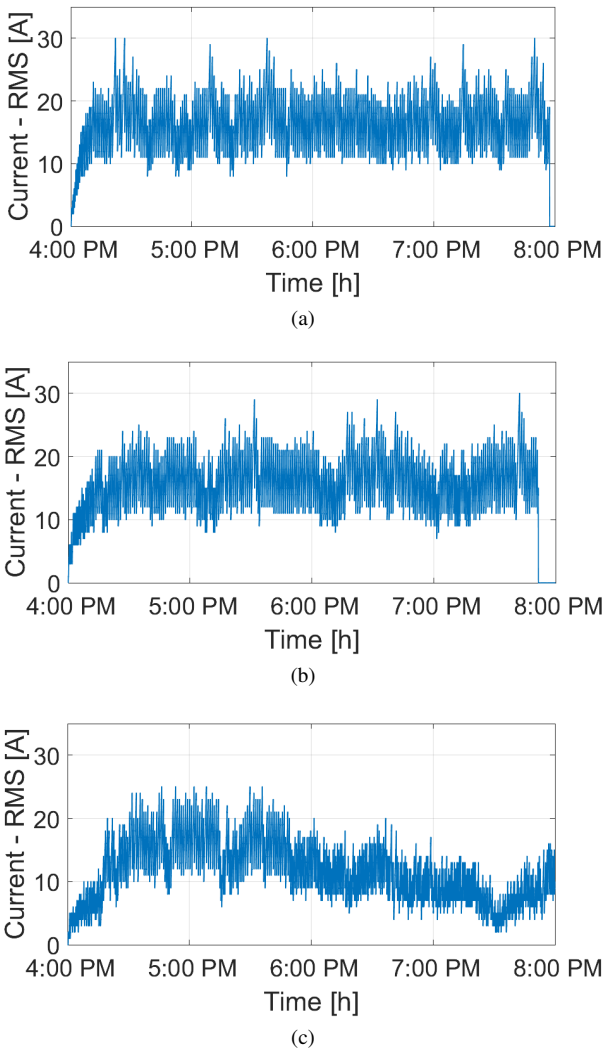

Figure 14: AIMD adopted EV charging currents, a) closest, b) intermediate, c) farthest nodes.

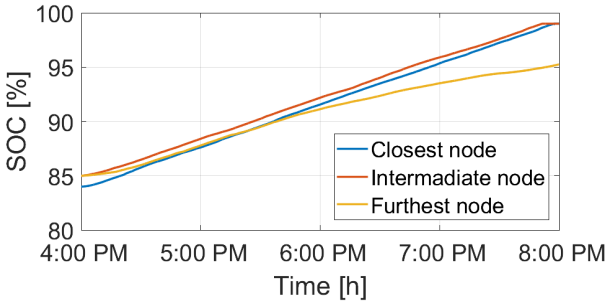

Figure 15: SOC variations of EVs at selected nodes.

References

[1] F. Erden, M. C. Kisacikoglu, and O. H. Gurec, "Examination of ev-grid integration using real driving and transformer loading data," in *Int. Conf. Elect. Electron. Eng.*, 2015, pp. 364–368.

[2] L. P. Fernandez, T. G. S. Roman, R. Cossent, C. M. Domingo, and P. Frias, "Assessment of the impact of plug-in electric vehicles on distribution networks," *IEEE Trans. Power Syst.*, vol. 26, no. 1, pp. 206–213, Feb 2011.

[3] S. Shafiee, M. Fotuhi-Firuzabad, and M. Rastegar, "Investigating the impacts of plug-in hybrid electric vehicles on power distribution systems," *IEEE Trans. Smart Grid*, vol. 4, no. 3, pp. 1351–1360, 2013.

[4] E. Veldman and R. A. Verzijlbergh, "Distribution grid impacts of smart

electric vehicle charging from different perspectives," *IEEE Trans. Smart Grid*, vol. 6, no. 1, pp. 333–342, 2015.

[5] E. Sortomme, M. M. Hindi, S. J. MacPherson, and S. Venkata, "Coordinated charging of plug-in hybrid electric vehicles to minimize distribution system losses," *IEEE Trans. Smart Grid*, vol. 2, no. 1, pp. 198–205, 2011.

[6] N. Leemput, F. Geth, J. Van Roy, A. Delnooz, J. Buscher, and J. Driesen, "Impact of electric vehicle on-board single-phase charging strategies on a flemish residential grid," *IEEE Trans. Smart Grid*, vol. 5, no. 4, pp. 1815–1822, 2014.

[7] K. Clement-Nyns, E. Haesen, and J. Driesen, "The impact of charging plug-in hybrid electric vehicles on a residential distribution grid," *IEEE Trans. Power Syst.*, vol. 25, no. 1, pp. 371–380, Feb 2010.

[8] O. Sundstrom and C. Binding, "Flexible charging optimization for electric vehicles considering distribution grid constraints," *IEEE Trans. Smart Grid*, vol. 3, no. 1, pp. 26–37, March 2012.

[9] P. Richardson, D. Flynn, and A. Keane, "Optimal charging of electric vehicles in low-voltage distribution systems," in *IEEE Power Energy Soc. General Meeting*, July 2012, pp. 1–1.

[10] F. Erden, M. C. Kisacikoglu, and N. Erdogan, "Adaptive V2G peak shaving and smart charging control for grid integration of PEVs," *Electric Power Compon. Syst.*, vol. 46, no. 13, pp. 1494–1508, 2018.

[11] S. Sojoudi and S. H. Low, "Optimal charging of plug-in hybrid electric vehicles in smart grids," in *IEEE Power Energy Soc. General Meeting*, July 2011, pp. 1–6.

[12] M. Restrepo, C. A. Cañizares, and M. Kazerani, "Three-stage distribution feeder control considering four-quadrant ev chargers," *IEEE Trans. Smart Grid*, vol. 9, no. 4, pp. 3736–3747, July 2018.

[13] M. C. Kisacikoglu, F. Erden, and N. Erdogan, "Distributed control of PEV charging based on energy demand forecast," *IEEE Trans. Ind. Informat.*, vol. 14, no. 1, pp. 332–341, Jan 2018.

[14] O. Ardakanian, S. Keshav, and C. Rosenberg, "Real-time distributed control for smart electric vehicle chargers: From a static to a dynamic study," *IEEE Trans. Smart Grid*, vol. 5, no. 5, pp. 2295–2305, Sep. 2014.

[15] S. Studli, E. Crisostomi, R. Middleton, and R. Shorten, "AIMD-like algorithms for charging electric and plug-in hybrid vehicles." Int. Elect. Veh. Conf., Mar. 2012, pp. 1–8.

[16] S. Studli, R. H. Khan, R. H. Middleton, and J. Y. Khan, "Performance analysis of an AIMD based EV charging algorithm over a wireless network," in *Australasian Univ. Power Eng. Conf.*, 2013, pp. 1–6.

[17] S. Studli, E. Crisostomi, R. Middleton, and R. Shorten, "A flexible distributed framework for realising electric and plug-in hybrid vehicle charging policies," *Int. J. Control*, vol. 85, pp. 1130–1145, Aug. 2012.

[18] M. Liu and S. McLoone, "Enhanced AIMD-based decentralized residential charging of EVs," *Trans. Inst. Meas. Control*, vol. 37, no. 7, pp. 853–867, 2015.

[19] V. Jacobson, "Congestion avoidance and control," in *Proc. Conf. Appl. Technol. Architectures, Protocols for Comput. Commun.*, Aug. 1988.

[20] M. Allman, V. Paxson, and E. Blanton, "TCP congestion control," *IETF RFC 5681*, September 2009.

[21] D. M. Chiu and R. Jain, "Analysis of the increase/decrease algorithms for congestion avoidance in computer networks," *Journal of Computer Networks and ISDN Systems*, vol. 17, no. 1, pp. 1–14, June 1989.

[22] E. Ucer, M. C. Kisacikoglu, and M. Yuksel, "Analysis of an Internet-inspired EV charging network in a distribution grid," in *IEEE/PES Transmiss. Distr. Conf.*, April 2018, pp. 1–5.

[23] E. Ucer, M. C. Kisacikoglu, and A. C. Gurbuz, "Learning EV integration impact on a low voltage distribution grid," in *IEEE Power Energy Soc. General Meeting*, Aug 2018, pp. 1–5.

[24] E. Ucer, M. C. Kisacikoglu, M. Yuksel, and A. C. Gurbuz, "An internet-inspired proportional fair EV charging control method," *IEEE Syst. J.*, 2019, in press.

[25] E. Ucer, M. C. Kisacikoglu, and M. Yuksel, "Analysis of AIMD algorithm for EV charging," in *ACM e-Energy*, 2019, accepted.

[26] ——, "Analysis of decentralized AIMD-based EV charging control," in *IEEE Power Energy Soc. General Meeting*, Aug 2019, pp. 1–5.

[27] S. Abourida, J. Bélanger, and V. Jalili-Marandi, "Real-time power system simulation: EMT vs. Phasor," OPAL-RT Technologies, Tech. Rep. opWP150620-sa-revA, Sep. 2016.

[28] S. Mojlish, N. Erdogan, D. Levine, and A. Davoudi, "Review of hardware platforms for real-time simulation of electric machines," *IEEE Transactions on Transportation Electrification*, vol. 3, no. 1, pp. 130–146, 2017.

[29] A. R. Malekpour and A. Pahwa, "Radial test feeder including primary and secondary distribution network," in *North American Power Symp.*, Oct 2015, pp. 1–9.

[30] Opal-RT Technologies. (2017) RT-LAB: distributed Real-Time platform ver. v11.2.2.108. [Online]. Available: https://www.opal-rt.com/software-rt-lab/

[31] (2019) Flexible Integration Laboratory for Distributed Energy Systems (FIELD) Facilities and Equipment. http://mck.people.ua.edu/facilities-and-equipment.html.

[32] S. Floyd, "Congestion control principles," *Internet Eng. Task Force Requests for Comments 2914*, September 2000.

[33] J. Nagle, "Congestion control in IP/TCP internetworks," *Internet Eng. Task Force Requests for Comments 896*, January 1984.